Steady-State Process Optimization with Guaranteed Robust Stability Under Parametric Uncertainty

YoungJung Chang and Nikolaos V. Sahinidis
Dept. of Chemical Engineering, Carnegie Mellon University, Pittsburgh, PA 15213

DOI 10.1002/aic.12530
Published online February 15, 2011 in Wiley Online Library (wileyonlinelibrary.com).

Interest in chemical processes that perform well in dynamic environments has led to the development of design methodologies that account for operational aspects of processes, including flexibility, operability, and controllability. In this article, we address the problem of identifying process designs that optimize an economic objective function and are guaranteed to be stable under parametric uncertainties. The underlying mathematical problem is difficult to solve as it involves infinitely many constraints, nonconvexities and multiple local optima. We develop a methodology that embeds robust stability constraints to steady-state process optimization formulations without any a priori *bifurcation analysis. We propose a successive row and column generation algorithm to solve the resulting generalized semi-infinite programming problem to global optimality. The proposed methodology allows modeling different levels of robustness, handles uncertainty regions without overestimating them, and works for both unique and multiple steady states. We apply the proposed approach to a number of steady-state optimization problems and obtain the least conservative solutions that guarantee robust stability.* © 2011 American Institute of Chemical Engineers *AIChE J,* 57: 3395–3407, 2011

Keywords: robust stability, steady-state optimization, generalized semi-infinite programming, parametric uncertainty, global optimization

Introduction

For decades, continuous operation of chemical processes has made steady-state optimization an important and popular design paradigm.[1] However, traditional steady-state optimization that ignores process dynamics may lead to designs that are overly conservative or not implementable.[2] As a result, there has been a steady interest in developing process design methodologies that address operational aspects of chemical processes, including flexibility[3–5] and operability.[6,7] For the same reason, the integration of process design and control has received much attention lately.[8–10] Recent approaches to steady-state process design with uncertainty and dynamics considerations include dynamic optimization approaches,[11] stochastic approaches,[12] and robust approaches.[13] A recent review of related advances can be found in Ricardez-Sandoval et al.[14]

This paper addresses the design of dynamic processes that are capable of returning to an original steady state after they are perturbed. This requirement is formally known as Lyapunov stability[15] and is one of the most desirable characteristics in the design of dynamic systems that are operated in some steady state. Clearly, the ability of a system to return to an original state is a function of the magnitude of the perturbation. Although designs that can

Correspondence concerning this article should be addressed to N. V. Sahinidis at sahinidis@cmu.edu.

reject large perturbations are desirable, ensuring such stability is very challenging.[16,17] Local stability conditions are considerably easier to enforce mathematically and embed in a design approach.[18–20] Still, the resultant design problems are challenging and often involve bilinear matrix inequalities.[21]

In the presence of uncertainty in the parameters that determine steady states, it is desirable to identify designs of chemical processes that remain stable over ranges of the uncertain parameters.[22] The ability of a system to do so is known as robust stability and is more difficult to ensure than stability at a point.[23,24] However, the importance of robust stability has stimulated extensive research in this field, including stability analysis of polytopic polynomials,[25] efficient suboptimal design approaches,[26,27] normal vector methods,[28,29] and robust eigenvalue placement.[30] Recently, a global optimization method was proposed to locate robustly stable steady-state solutions to biochemical process optimization problems.[31] This approach successfully identified metabolic network redesigns that are robustly stable under predefined general model uncertainties. However, in the case of parametric uncertainty alone, this approach can produce conservative solutions.[32]

In this article, we build on the approach of Chang and Sahinidis[31] and develop a methodology to handle parametric uncertainties in a way that does not lead to conservative designs. The methodology proposed in this article relies on an analytical approach to enforce robust stability in steady-state optimization problems. The resulting formulation corresponds to a bilevel optimization problem that is intuitive but difficult to solve.[33] Therefore, the bilevel program is converted to an equivalent single-level program with infinitely many stability constraints by using necessary and sufficient algebraic conditions for stability. The resulting semi-infinite program is solved to global optimality by identifying a finite subset of stability constraints that will suffice to solve the problem.

In contrast to prior approaches, our methodology requires no a priori bifurcation analysis of the system while providing a deterministic guarantee for the least conservative stable steady-state solutions. The uncertainty region is handled directly with no need to overestimate it by a smooth surface. Moreover, our approach can handle multiple steady states and limit cycles, and can be extended to account for more general uncertainties in the process model.

The remainder of this article is structured as follows. In the next section, we define the problem of interest and formulate steady-state optimization problems with robust stability constraints as mathematical programs. A natural bilevel formulation is reformulated into a generalized semi-infinite programming problem. Then, a successive row and column generation solution algorithm is developed to solve the resulting semi-infinite programs. The proposed methodology is extended to account for more general model uncertainties and limit-cycle solutions. The broad applicability of the proposed methodology is illustrated by investigating six different problems. Finally, conclusions are drawn and future research directions are discussed.

Robust Stability under Parametric Uncertainty

Problem formulation

We consider a dynamic system described by a set of ordinary differential equations

$$\frac{dx}{dt} = f(p, u; x), \tag{1}$$

where x is a vector of dependent (state) variables in a compact set $X \subset \mathbb{R}^n$, u is a vector of independent (design) variables in a compact set $U \subset \mathbb{R}^m$, and p is a vector of uncertain parameters in a bounded neighborhood N about its nominal value $\bar{p}$. In general, X is defined by design specifications.

The variations in the system can be classified into process uncertainties in u and model uncertainties in p.[34] Bounded disturbances in design variables can be translated into parametric uncertainties in most cases. In particular, a variable u' that is under a disturbance, can be decomposed as a sum of a certain portion u and an uncertain portion p' with a nominal value of zero. While we can decompose u' as $u + p'$ in the case of an absolute disturbance, we can decompose u' as $u(1 + p')$ in the case of a relative disturbance.

The steady state of system (1) is characterized by setting the left-hand side to 0. For simplicity, we assume that there is a unique steady state in X for any (p, u) pair, but the approach presented here can be used for the case with multiple steady states as shown later in the section on the solution algorithm. According to the Lyapunov linearization theorem,[35] all the eigenvalues of the Jacobian $Df(p, u; x) = \frac{\partial f}{\partial x}$ must have negative real parts for local stability at equilibrium.

Let x be the steady state at $\bar{p}$ for a given u. To ensure robust stability of x, we require every steady state y corresponding to any p in N to be locally stable. With λ denoting any eigenvalue of $Df(p, u;y)$ and $\Re(\lambda)$ its real part, this condition can be written as:

$$\left.\begin{array}{ll} \max_{p,y} & \Re(\lambda) \\ \text{s.t.} & f(p, u; y) = 0 \\ & p \in N \\ & y \in Y(u, x) \end{array}\right\} < 0. \tag{2}$$

Here, $Y(u,x)$ signifies the neighborhood of x in the state space where robust stability matters. If the effect of parametric uncertainty onto state space is completely unknown, prescribing $Y(u,x)$ in a way that overestimates the set of all physically possible steady states of the system may lead to conservative designs and even make (2) infeasible.

Condition (2) can be used as a stability constraint in the context of a design formulation, in which one would like to maximize an economic merit function $\phi(p, u; x)$. One can optimize for the worst-case or expected objective value or minimize the variance of the objective value. To keep the presentation simple, we choose to optimize ϕ evaluated at the median $p = \bar{p}$. Embedding robust local stability conditions into the larger optimization formulation results in the following bilevel programming problem:

$$\max_{u,x} \quad \phi(\bar{p}, u; x) \tag{3}$$

$$\text{s.t.} \quad f(\bar{p}, u; x) = 0 \tag{4}$$

$$\left\{\begin{array}{ll}\max_{p,y} & \Re(\lambda)\\ \text{s.t.} & f(p,u;y)=0,\ p\in N,\ y\in Y(u,x)\end{array}\right\}<0, \qquad (5)$$
$$x\in X,\quad u\in U.$$

The formulation seeks to identify a steady state (4) that optimizes the nominal performance measure (3) while guaranteeing stability on all of the steady states induced in the neighborhood of the uncertain parameters (5). The inner optimization problem in the above formulation will be recast as infinitely many constraints of the form $r(p, u; y) > 0$ derived from equivalent stability conditions.[36] Computing the characteristic equation of $Df(p, u; x)$:

$$\lambda^n + v_1(p,u;x)\lambda^{n-1} + \cdots + v_{n-1}(p,u;x)\lambda + v_n(p,u;x) = 0$$

and applying the Routh-Hurwitz test[37] symbolically, we obtain the inequalities:

$$r_i(p,u;x) = \begin{vmatrix} v_1 & 1 & 0 & 0 & 0 & 0 & \cdots & 0\\ v_3 & v_2 & v_1 & 1 & 0 & 0 & \cdots & 0\\ v_5 & v_4 & v_3 & v_2 & v_1 & 1 & \cdots & 0\\ \vdots & \vdots & \vdots & \vdots & \vdots & \vdots & \ddots & \vdots\\ v_{2i-1} & v_{2i-2} & v_{2i-3} & v_{2i-4} & v_{2i-5} & v_{2i-6} & \cdots & v_i \end{vmatrix} > 0$$

for $i = 1,\ldots,n$.[38] The resulting single-level optimization problem is:

$$\begin{array}{lll}(\mathrm{P}) & \max & \phi(\bar{p},u;x)\\ & \text{s.t.} & f(\bar{p},u;x)=0,\\ & & r(p,u;y)>0\\ & & \quad \forall (p,y)\in\{(q,w)\in N\times Y(u,x)|f(q,u;w)=0\},\\ & & x\in X,\quad u\in U.\end{array}$$

The robust stability condition (5) is different from the one that was used in Chang and Sahinidis[31]:

$$\left\{\begin{array}{ll}\max_{p,y} & \Re(\lambda)\\ \text{s.t.} & p\in N\\ & y\in Y'(x)\end{array}\right\}<0, \qquad (6)$$

in that (6) allows y to change independent of (p, u) to account for both parametric and nonparametric uncertainties. Therefore, the extension of the row-generation solution methodology proposed therein[31] to the present context is challenging due to the need to accommodate the equilibrium constraints in the inner stability constraint of P. We overcome this challenge through an algorithm based on row and column generation. Before embarking on algorithm development, we use an example to illustrate the modeling aspects of the proposed approach and, in particular, the derivation of the infinite stability constraints.

Illustrative example: Brusselator model

Consider the following set of elementary chemical reactions[39]:

$$\begin{aligned} \mathrm{A} &\xrightarrow{k_1} \mathrm{X},\\ \mathrm{B}+\mathrm{X} &\xrightarrow{k_2} \mathrm{Y}+\mathrm{C},\\ 2\mathrm{X}+\mathrm{Y} &\xrightarrow{k_3} 3\mathrm{X},\\ \mathrm{X} &\xrightarrow{k_4} \mathrm{D}, \end{aligned}$$

where A and B are reagents, C and D are products, and X and Y are intermediary chemical species. Material balances for X and Y are:

$$\frac{dC_\mathrm{X}}{dt} = k_1C_\mathrm{A} - k_2C_\mathrm{B}C_\mathrm{X} + k_3C_\mathrm{X}^2C_\mathrm{Y} - k_4C_\mathrm{X},$$
$$\frac{dC_\mathrm{Y}}{dt} = k_2C_\mathrm{B}C_\mathrm{X} - k_3C_\mathrm{X}^2C_\mathrm{Y}.$$

Since the precise determination of the rate of transformation between intermediates is difficult, we assume that the value of k_3 is uncertain. We further assume that the concentration of B is under disturbances. By letting $\tau = k_4t$, $x_1 = \frac{k_4C_\mathrm{X}}{k_1C_\mathrm{A}}$, $x_2 = \frac{k_4C_\mathrm{Y}}{k_1C_\mathrm{A}}$, $p_1 = \frac{k_3^2k_3C_\mathrm{A}^2}{k_4^3}$, and $u' = \frac{k_2C_\mathrm{B}}{k_4}$, the model can be recast in dimensionless form:

$$\frac{dx_1}{d\tau} = 1 - (u'+1)x_1 + p_1x_1^2x_2,$$
$$\frac{dx_2}{d\tau} = u'x_1 - p_1x_1^2x_2.$$

Note that p_1 and u' are uncertain. Decomposing u' into certain and uncertain contributions $u + p_2$, we obtain a dynamic system in the form of (1) with:

$$f_1(p,u;x) = 1 - (u+p_2+1)x_1 + p_1x_1^2x_2,$$
$$f_2(p,u;x) = (u+p_2)x_1 - p_1x_1^2x_2.$$

We assume that $X = (0, 10] \times (0, 10]$, $U = [1, 5]$, $\bar{p} = (3, 0)$, $N = \bar{p} + [-0.1, 0.1] \times [-0.1, 0.1]$, and $Y(x) = X$. The stability conditions for the model are $\det(Df) > 0$ and $\mathrm{trace}(Df) < 0$ where

$$Df(p,u;x) = \begin{bmatrix} -(u+p_2) - 1 + 2p_1x_1x_2 & p_1x_1^2\\ (u+p_2) - 2p_1x_1x_2 & -p_1x_1^2 \end{bmatrix}.$$

Since $\det(Df)$ is always positive, the only remaining stability constraint is

$$r(p,u;y) = -\mathrm{trace}(Df|_y) = p_1y_1^2 + (u+p_2) + 1 - 2p_1y_1y_2 > 0.$$

If the steady-state performance measure is the production rate of C, the overall productivity optimization problem with robust stability constraints becomes:

$$\begin{array}{ll}\max & ux_1\\ \text{s.t.} & 1-(u+1)x_1+3x_1^2x_2=0,\\ & ux_1-3x_1^2x_2=0,\\ & p_1y_1^2+(u+p_2)+1-2p_1y_1y_2>0\\ & \forall(p,y)\in\left\{(q,w)\left|\begin{array}{l}1-(u+q_2+1)w_1+q_1w_1^2w_2=0,\\ (u+q_2)w_1-q_1w_1^2w_2=0,\\ q\in N,\quad w\in X.\end{array}\right.\right\},\\ & x\in X,\quad u\in U.\end{array}$$

In addition to nonconvexities in equality constraints, the model involves an infinite number of constraints that enforce the stability requirement. A specialized algorithm is developed in the next section to address these two challenges.

Solution Algorithm

The stability conditions in P must be satisfied by infinitely many steady-state points. By dropping all the stability constraints, we obtain a relaxation whose solution is an upper bound on the optimal value of P. The main idea is to iteratively introduce a small number of stability constraints to strengthen this relaxation and, eventually, arrive at a solution that satisfies all the stability constraints of P. For simplicity of the presentation, we assume that Y is a static neighborhood of x.

The solution (u^0, x^0) to the initial relaxation problem is not likely to satisfy the robust stability condition. For instance, solving the Brusselator example after ignoring all the stability constraints produces the solution:

$$u^0 = 5, \quad x^0 = (1, 5/3),$$

which does not satisfy the stability condition at $p = \overline{p}$ and is, therefore, unstable.

Let $p^0 \in N$ produce an unstable steady state in $Y(x^0)$ under the design u^0. By noticing that the steady state $y^0(p^0, u) \in Y(x)$ corresponding to any solution (u, x) must satisfy the stability condition, we can introduce the following set of constraints to cut off the current solution (u^0, x^0):

$$f(p^0, u; y^0) = 0, \quad r(p^0, u; y^0) > 0, \quad y^0 \in Y(x).$$

Note that p^0 is a constant vector but y^0 is a vector of variables. For the illustrative example, these constraints for $p^0 = \overline{p}$ correspond to

$$\begin{aligned} f_1(p^0, u; y^0) &= 1 - (u+1)y_1^0 + 3(y_1^0)^2 y_2^0 = 0, \\ f_2(p^0, u; y^0) &= u y_1^0 - 3(y_1^0)^2 y_2^0 = 0, \\ r(p^0, u; y^0) &= 3(y_1^0)^2 + u + 1 - 6y_1^0 y_2^0 > 0. \end{aligned}$$

At iteration K of the algorithm, let (u^K, x^K) be the solution of the relaxation problem:

$$\begin{aligned} \text{(R)} \quad \max \quad & \phi(\bar{p}, u; x) \\ \text{s.t.} \quad & f(\bar{p}, u; x) = 0, \\ & r(\bar{p}, u; x) > 0, \\ f(p^k, u; y^k) = 0, \quad & k = 0, \ldots, K-1, \qquad (7) \\ r(p^k, u; y^k) > 0, \quad & k = 0, \ldots, K-1, \qquad (8) \\ x \in X, \quad & u \in U, \\ y^k \in Y(x), \quad & k = 0, \ldots, K-1. \end{aligned}$$

Since (7) and (8) are merely a subset of the infinitely many stability constraints of P, the solution to R may not satisfy some of the stability constraints that are not considered yet. Therefore, we solve the following separation problem to find p^K that corresponds to an unstable steady state:

$$\begin{aligned} \text{(S)} \quad \min \quad & \sum_i b_i r_i(p, u^K; y) \\ \text{s.t.} \quad & f(p, u^K; y) = 0, \\ & \sum_i b_i \le 1, \\ & p \in N, \quad y \in Y(x^K), \\ & b_i \in \{0, 1\} \quad \forall i. \end{aligned}$$

Here, binary variables b are used to isolate the maximally violated stability constraint. If the optimal value of S is 0, this provides a proof that (u^K, x^K) is a robustly stable design. On the other hand, if the objective value to S is negative, then this implies that the current solution is not robustly stable. In the latter case, we introduce stability cuts for p^K to the relaxation problem, increment K by one, and continue with solving the updated relaxation. Unlike a similar approach for the back-off flexibility design that introduced multiple violates depending on the number of constraints,[40,41] we introduce a single violate at each iteration for improved computational efficiency.

Revisiting the Brusselator example, the algorithm solved the problem in two iterations within one CPU second. The robustly stable steady-state solution to this problem is

$$u = 3.800, \quad x = (1, 1267).$$

The validity of this solution can be checked analytically as follows. If (p, u) is fixed, the Brusselator model has a unique steady state $x = \left(1, \frac{u+p_2}{p_1}\right)$. At this steady state, the robust stability condition can be reduced to $u + p_2 < p_1 + 1$, $\forall p \in N$. This inequality can be simplified to a single inequality $u < 3.8$. Since the objective function is maximizing $ux_1 = u$, the largest allowable value of u must be optimal, in agreement with the computationally obtained solution.

Multiple steady states with different stability trends

The proposed strategy solves the robust stability problem if there is a unique steady-state for each (p, u) pair. The strategy is also applicable to the multiple steady-state case without modification if all the steady states within $Y(x)$ have consistent stability trends, by which we mean that the steady states corresponding to a fixed (p, u) are either all stable or all unstable. In this section, we extend the solution method for the case of multiple steady states with inconsistent stability trends.

At iteration K of the algorithm, assume that the relaxation solution is (u^K,x^K) and there are two steady states y^s, $y^u \in Y(x^K)$ both corresponding to a $p^K \in N$. As the superscript implies, y^s corresponds to a stable steady state and y^u to an unstable one. In this case, introducing the stability cut at p^K into the relaxation problem due to y^u does not eliminate the current solution, because $y^K = y^s$ satisfies the newly inserted stability condition. As a result, the same solution (u^K, x^K) repeats as relaxation solution.

Accepting or rejecting the repeating solution depends on the extent of robustness in stability that we seek. If all the multiple steady states in $Y(x)$ must be stable, then we discard the current solution (u^K, x^K). In the special case of $X \subseteq Y(x)$, we can discard (u^K, x) for all $x \in X$. If one stable steady state suffices for each $p \in N$ (less robustness), we search for a $q^K \in N$ that gives rise to unstable steady states

only. This step requires the solution of the following problem at each grid point q in a discretization of N:

$$\begin{aligned}(\text{F1}) \quad \max \quad & z \\ \text{s.t.} \quad & f(q,u^K;y)=0, \\ & r_i(q,u^K;y)\geq z \quad \forall i, \\ & y\in Y(x^K).\end{aligned}$$

If there is any q^K such that the optimal value to this problem is negative, then we substitute the stability cuts for p^K with those for q^K in the relaxation problem and repeat. Otherwise, we accept the solution and terminate.

Finally, we consider a design for which an uncertainty realization does not correspond to any steady state. To ensure stationary operation of process, the design must be rejected. We detect such a design by solving the following feasibility problem at each grid point q in a discretization of N:

$$\begin{aligned}(\text{F2}) \quad \min \quad & z \\ \text{s.t.} \quad & -z\leq f(q,u^K;y)\leq z, \\ & y\in Y(x^K).\end{aligned}$$

If there is any q^K such that the optimal value to the problem is positive, we reject the current design u^K by introducing the following constraints into the relaxation problem:

$$f(q^K,u;y^K)=0$$

Otherwise, we accept the solution and terminate.

The use of a simple adaptive scheme for the discretization of N was sufficient for the problems F1 and F2 solved in this study. We first solve these problems on a coarse mesh, and check their optimal values and their sensitivities. Since the optimal values are continuous for both F1 and F2, we refine the mesh only if the sensitivity information suggests a qualitative change of the optimal value in between the mesh points (e.g., a sign flip for F1). More elaborate discretization schemes that have been developed for building surrogate models (cf., Brendel and Marquardt[42]) may be necessary for more complex problems. Parametric programming approaches can also be used to assist or replace the discretization-based feasibility check.[43]

Implementation

Stability constraints become more complex if the Jacobian matrix has many nonzero elements. Although the Jacobian is sparse in general, it is worth keeping the number of its nontrivial elements to a minimum using steady-state conditions. For example, the left-hand-side of a balance $p_1x_1x_2 - p_2x_2 = 0$ has zero sensitivity to $x_2 > 0$ at a steady state, but automatic differentiation may not identify this implicit insensitivity. Therefore, we solved the following problems for each nontrivial Jacobian element Df_{ij}:

$$\begin{aligned}\min/\max \quad & Df_{ij} \\ \text{s.t.} \quad & f(p,u;x)=0, \\ & x\in X,\ u\in U.\end{aligned}$$

If the minimum and maximum values of Df_{ij} are equal, we fix Df_{ij} at this value. We also simplify the symbolic expressions in the variable Jacobian elements by using $f = 0$ whenever possible.

In the proposed algorithm, the separation problem S, a mixed-integer nonlinear program, must be solved to global optimality to ensure robust stability. Solving the relaxation problem to global optimality is also preferred. To globally solve the nonconvex, nonlinear optimization problems, we employed the BARON global optimization system that implements the branch-and-reduce global optimization strategy.[44,45] Our algorithm was implemented under the GAMS modeling system. All runs reported herein were on a Linux computer with 2.8 GHz Intel Pentium quad-core processor and 8 GB RAM.

Extensions

Robust stability for general model uncertainties

We extend formulation P to account for the general model uncertainties that are addressed in Chang and Sahinidis[31] to obtain a more comprehensive model. We assume that, for each (p, u), the real steady state stays in $[x(1 - \delta_1) - \delta_2,\ x(1 + \delta_1) + \delta_2]$ where x is the corresponding solution to the mathematical model, and that the Jacobian of the model can be used to determine the local stability of these unsure real steady states. We assume that δ_1 and δ_2 are nonnegative constant vectors and only one of them is nonzero (either all relative or all absolute). The resulting optimization problem is

$$\begin{aligned}(\text{P}') \quad \max \quad & \phi(\bar{p},u;x) \\ \text{s.t.} \quad & f(\bar{p},u;x)=0, \\ & r(p,u;y)>0 \quad \forall (p,y)\in\Upsilon, \\ & x\in X, \quad u\in U,\end{aligned}$$

where

$$\Upsilon=\left\{(q,w)\left|\begin{array}{l} f(q,u;v)=0, \\ v(1-\delta_1)-\delta_2\leq w\leq v(1+\delta_1)+\delta_2, \\ q\in N, \quad v\in Y(u,x)\end{array}\right.\right\}.$$

Note that P is a special case for which $\delta_1 = \delta_2 = 0$, assuming parametric uncertainty only. The solution strategy proposed in this work can be applied to solve P′ with modifications in R and S as follows:

$$\begin{aligned}(\text{R}') \quad \max \quad & \phi(\bar{p},u;x) \\ \text{s.t.} \quad & f(\bar{p},u;x)=0, \\ & r(\bar{p},u;x)>0, \\ & f(p^k,u;y^k)=0, \quad k=0,\ldots,K-1, \\ & r(p^k,u;y^k(1+\delta_1^k)+\delta_2^k)>0, \quad k=0,\ldots,K-1, \\ & x\in X, \quad u\in U, \\ & y^k\in Y(x), \quad k=0,\ldots,K-1.\end{aligned}$$

$$\begin{aligned}(\text{S}') \quad \min \quad & \sum_i b_i r_i(p,u^K;w) \\ \text{s.t.} \quad & f(p,u^K;y)=0, \\ & y(1-\delta_1)-\delta_2\leq w\leq y(1+\delta_1)+\delta_2 \\ & \sum_i b_i\leq 1, \\ & p\in N, \quad y\in Y(x^K), \\ & b_i\in\{0,1\} \quad \forall i.\end{aligned}$$

By solving S′, we find an optimal (p^K, y^K, w^K) and compute either $\delta_1^K = w^K/y^K - 1$ or $\delta_2^K = w^K - y^K$.

Limit-cycle optimization with stability

Unsteady state operation of oscillating processes has been of interest to chemical engineers because dynamic operation sometimes increases productivity.[46,47] The proposed formulation and methodology can be also applied to find stable limit-cycle solutions by using the concept of Poincaré first return map.[48] Here, we sketch the steps to derive formulation P for limit-cycle cases.

We approximate the limit cycle of period τ by a truncated Fourier series representation:

$$x(t) = a_0 + \sum_{i=1}^{v} \left[a_i \cos\left(\frac{2\pi i t}{\tau}\right) + b_i \sin\left(\frac{2\pi i t}{\tau}\right) \right]$$

where a, b, and τ are unknown, which will be determined by enforcing $dx/dt = f(p, u; x)$ on a set of μ time points that are uniformly distributed within $(0, \tau]$:

$$\frac{dx}{dt}\left(\frac{m\tau}{\mu}\right) = f\left(p, u; x\left(\frac{m\tau}{\mu}\right)\right), \quad m = 1, \ldots, \mu.$$

In the time domain harmonic balance technique,[49] we choose $\mu = 2v + 1$ and additionally set $a_1 = 0$ and $\|b_1\| > 0$ (phase-fixing).

After obtaining the periodic solution $x(t)$, we derive its stability conditions via a monodromy matrix M that satisfies the following initial-value problem:

$$M(0) = I_n, \quad \frac{dM}{dt} = Df(p, u; x)M,$$

which can be integrated by a time discretization scheme. For an autonomous system, the transition matrix $M(\tau)$ always has an eigenvalue of $+1$. For the limit cycle to be stable, the remaining $n-1$ eigenvalues must be smaller than unity in modulus.[50] If the characteristic polynomial of $M(\tau)$ is $(\lambda-1)\psi(\lambda)$, this Schur stability condition on $\psi(\lambda)$ is equivalent to requiring its transformation such as $(\lambda-1)^{n-1}\psi\left(\frac{\lambda+1}{\lambda-1}\right)$ to be Hurwitz stable.[51] We can then employ the techniques described earlier in this study and Chang and Sahinidis[36] to construct equivalent algebraic conditions for the Hurwitz stability of the resulting polynomial, and embed them into the limit-cycle productivity optimization problem.

Applications

In this section, we consider six problems to demonstrate how our formulation and solution algorithm result in the least conservative robustly stable designs that are possible for these problems.

One-dimensional autocatalytic process

Consider an autocatalytic chemical reaction model

$$\frac{dx}{dt} = u' - 6x + \frac{10x^2}{1+x^2}.$$

This model has two saddle-node bifurcation points at $u' = 0.897$ and $u' = 1.021$. In the interval between these bifurcation points, there are three steady states, two stable, and one unstable. Outside this interval, there exists a unique stable steady state. The bifurcation diagram for this process is provided in Figure 1.

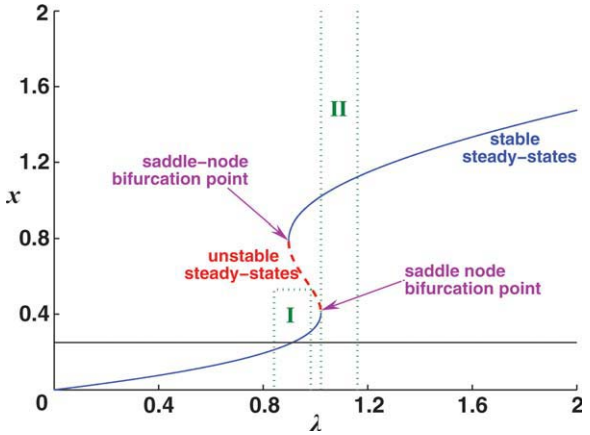

Figure 1. Bifurcation diagram for the autocatalytic chemical model.

[Color figure can be viewed in the online issue, which is available at wileyonlinelibrary.com.]

Now, let us consider the following steady-state optimization problem:

$$\begin{aligned} \min \quad & x \\ \text{s.t.} \quad & 0 = u' - 6x + \tfrac{10x^2}{1+x^2}, \\ & x \in [0.25, 2],\ u' \in [0, 9118, 2]. \end{aligned}$$

We assume that u' can fluctuate about its mean value, thus decompose u' to $u + p$. We want the solution to be robustly stable for any $p \in [-0.07, 0.07]$. Because of the two stability boundaries on the parameter space, normal vector methods would give the solution of $u = 1.091$. Our method identified the same solution in four iterations by requiring all the multiple steady states within $Y(x) = \mathbb{R}_+$ to be stable. This solution is depicted as the unbounded region II that touches a saddle-node bifurcation point in Figure 1.

If a realistic bound for the state exists under the disturbance in u', namely $Y(x) = [x - 0.28, x + 0.28]$, then the proposed algorithm gives the optimal solution of $(u, x) = (0.9118, 0.25)$, which is shown as the box I that touches an unstable steady-state curve in Figure 1. Even if $Y(x) = \mathbb{R}_+$, the same solution qualifies as the least robust solution as discussed in the subsection on multiple steady states with different stability trends. This solution is unattainable by normal vector methods unless we know that the bifurcation point $u' = 0.897$ is irrelevant to the optimal solution.

Reactor design problems

Fermentation Process in CSTR. A simple CSTR fermenter model has been under extensive study for its bifurcation analysis[52] and process flowsheet design.[53] The essence of its rich dynamics can be investigated by the following two-dimensional model[54,29]:

$$\frac{dC_X}{dt} = -\frac{F}{5.13\pi}C_X + C_S \exp(-C_S/0.12)C_X$$
$$\frac{dC_S}{dt} = \frac{F}{5.13\pi}(C_{Sf} - C_S) - \frac{C_S \exp(-C_S/0.12)}{5.4 + 180C_S}C_X$$

where C_X and C_S are concentrations of biomass and substrate, respectively. The feed flow rate F and all of the concentrations

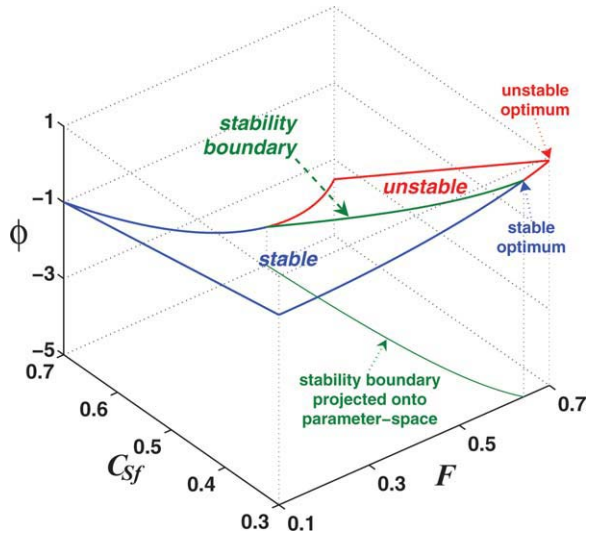

Figure 2. Steady states and their corresponding objective values for the open-loop fermentation process in CSTR.

[Color figure can be viewed in the online issue, which is available at wileyonlinelibrary.com.]

are strictly positive, and the feed substrate concentration C_{Sf} is bounded within [0.3, 0.7]. Naturally, $C_S \le C_{Sf}$. We would like to determine F and C_{Sf} so as to maximize the operating profit:

$$\phi_1 = \frac{10F}{97}\left[5C_X - \left(10.8\frac{1-C_{Sf}}{0.7} + 200\frac{C_{Sf}-0.3}{0.7}\right)\right].$$

Ignoring the trivial steady state of zero biomass ($C_X = 0$ and $C_S = C_{Sf}$), the steady-state condition of the first equation can be rearranged to:

$$\frac{F}{5.13\pi} = \mu(C_S) \equiv C_S \exp(-C_S/0.12).$$

Notice that $\mu(C_S)$ is monotonically increasing when $C_S < 0.12$ and decreasing when $C_S > 0.12$. As a result, the global maximum of $F \le 0.6156\pi/e$ is attained at $C_S = 0.12$, and there are two distinct solutions $C_S^l < 0.12$ and $C_S^u > 0.12$ for each $F \in (0, 0.6156\pi/e)$. Consider the Jacobian of the right-hand side at a steady state:

$$Df = \begin{bmatrix} 0 & C_X\mu' \\ -\frac{\mu}{5.4+180C_S} & -\mu - \frac{C_X\mu'}{5.4+180C_S} + \frac{180C_X\mu}{(54+180C_S)^2} \end{bmatrix}.$$

Its determinant is negative and the steady state is unstable whenever $\mu' = d\mu/dC_S$ is negative, which is always the case for C_S^u. Therefore, we restrain $C_S \le 0.12$.

Table 1. Robust Solutions at Different Levels of Uncertainty for the Fermentation Process in CSTR

ρ	(F, C_{Sf})	ϕ_1	Iteration #
0	(0.643, 0.3)	0.685	1
0.001	(0.603, 0.3)	0.566	3
0.002	(0.587, 0.3)	0.524	3
0.003	(0.575, 0.3)	0.494	3
0.004	(0.565, 0.3)	0.471	3
0.005	(0.557, 0.3)	0.451	3

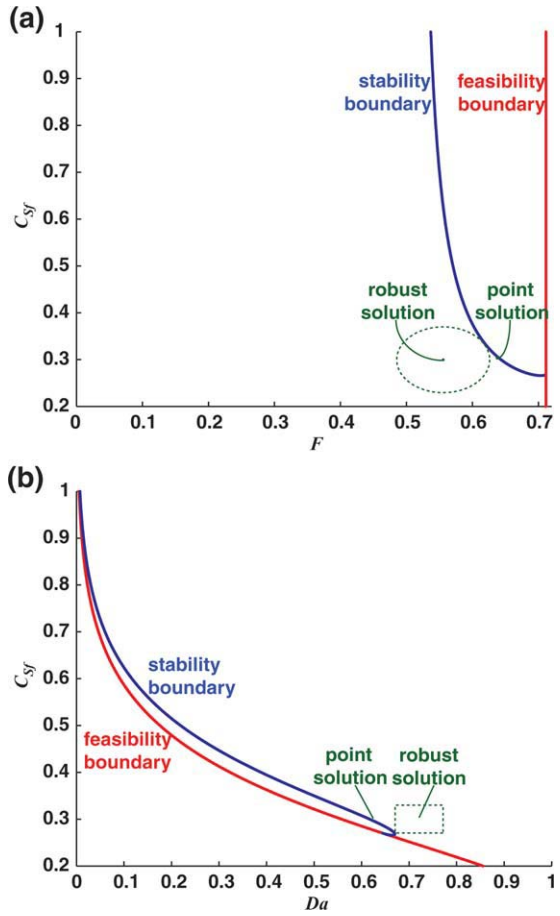

Figure 3. Robust solutions on different neighborhoods of uncertainty N_1 with $\rho = 0.005$ (a) and N_2 (b) for the open-loop fermentation process in CSTR.

[Color figure can be viewed in the online issue, which is available at wileyonlinelibrary.com.]

The steady states satisfying all these conditions are shown in Figure 2, along with the corresponding objective function values. Stable and unstable steady states are separated by a stability boundary in this case. As observed in the figure, the maximum objective value is achieved at an unstable steady state. Here, we assume that F and C_{Sf} are under operational disturbances and decompose them to $u = (\overline{F}, \overline{C}_{Sf})$ and $p = (\delta F, \delta C_{Sf})$. To enforce stability that is robust to uncertainties in p, we consider robustness regions of two different shapes:

$$N_1 =: (\delta F)^2 + (\delta C_{Sf})^2 \le \rho,$$
$$N_2 =: |\delta C_{Sf}| \le 0.03; |\delta Da| \le 0.05,$$

where $Da = \frac{5.13\pi}{F} C_{Sf} \exp(-C_{Sf}/012)$.

In this example, $Y(x)$ is set equal to the entire region X. With ρ varying from 0 to 0.005, the optimal solutions shown in Table 1 are obtained for N_1. All five robust solutions were obtained in 2.0 CPU s. For the other neighborhood N_2, $\phi_1 = 0.436$ is attained at $(C_{Sf}, Da) = (0.3, 0.721)$ in four iterations and 2.3 s. These solutions are shown in Figure 3. In this figure, the boundary between stable and unstable steady states is shown in solid blue. Feasibility boundaries correspond to the combination of parameters beyond which no steady-state solution exists.

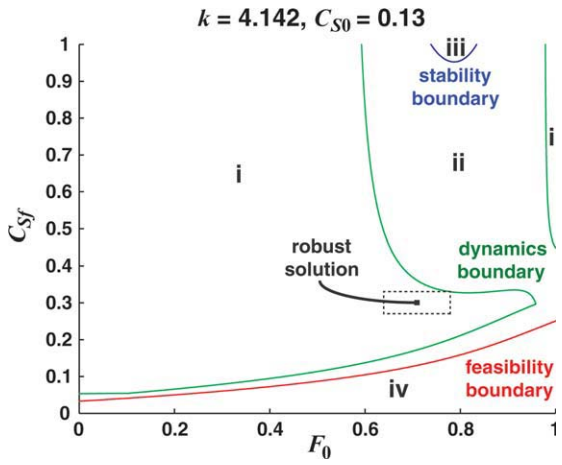

Figure 4. Robust solution for the closed-loop fermentation process in CSTR.

[Color figure can be viewed in the online issue, which is available at wileyonlinelibrary.com.]

We next consider closing the open-loop system by adding a feedback proportional controller $F = F_0 + G(C_{S0} - C_S)$ to the process, where F_0 is the feed flow rate under no control action, $G > 0$ the gain of the controller, and C_{S0} the set point for substrate concentration in the tank.[55] This time, we seek to determine F_0, C_{Sf}, G, and C_{S0} that maximize the profit function:

$$\phi_2 = 0.5C_X F + 7.03F - 27.03C_{Sf}F - 0.01G,$$

while demanding that the closed-loop eigenvalues are smaller than $-1/60$ for all possible realizations of uncertain parameters in the following box:

$$N_3 =: |\delta F_0| \le 0.07; |\delta C_{Sf}| \le 003.$$

Note that the requirement on the eigenvalues is equivalent to requiring $Df + \frac{1}{60}I$ to be a stable matrix.

At a steady state, there should be no control action such that $C_{S0} = C_S$ and $F = F_0$. Then, the first steady-state equation becomes $\frac{F_0 + GC_{S0}}{5.13\pi} = \mu(C_S) + \frac{G}{5.13\pi}C_S$. If $G \ge 5.13\pi/e^2$, this equation can have only one solution. Otherwise, the right-hand side has a local maximum between 0.12 and 0.24, and a local minimum beyond 0.24. Therefore, there could be three solutions to the equation depending on the value of the left-hand side. Interestingly, all the C_S values between these two extrema give rise to unstable steady-state behavior due to the negative determinant of Jacobian matrix. Therefore, we introduce $G \ge 5.13\pi/e^2$ and drop the condition of $C_S \le 0.12$ in the open-loop problem.

Table 2. Model Constants for the Jacketed CSTR

Parameter	Value	Parameter	Value
V	$\frac{\pi}{2}D^3$	V_j	$0.25V$
ρ	50	ρ_j	62.3
C_p	0.75	C_{pj}	1
T_f	{525, 530, 535}	T_{fj}	530
ΔH	−30000	$\frac{E}{R}$	15106.5
U	{145, 150, 155}	A	$\frac{9\pi}{4}D^2$
k_0	7.08×10^{10}	C_{Af}	{0.45, 0.50, 0.55}

The proposed algorithm returned the solution (F_0, C_{Sf}, G, C_{S0}) = (0.709, 0.3, 41.42, 0.13) with the objective value of 0.929 in two iterations and 2.2 CPU s. Figure 4 shows that the uncertainty box around the solution touches the required first-order dynamics boundary. The boundary between stable and unstable steady states is shown in solid blue, and the boundary between fast and slow convergence rates is shown in solid green. Feasibility boundary is shown in solid red. Area i corresponds to stable and fast, ii to stable but slow, and iii to unstable steady states. Area iv corresponds to parameter values that do not correspond to any steady state.

Exothermic First-Order Reaction in CSTR. A CSTR for an exothermic irreversible reaction is modeled as in[56]:

$$\frac{dC_A}{dt} = \frac{F}{V}(C_{Af} - C_A) - k_0 \exp\left(\frac{-E}{RT}\right)C_A$$
$$\frac{dT}{dt} = \frac{F}{V}(T_f - T) - \frac{\Delta H}{\rho C_p}k_0 \exp\left(\frac{-E}{RT}\right)C_A - \frac{UA}{\rho C_p V}(T - T_j)$$

where C_A is the concentration of the reactant, T is the reactor temperature, and T_j is the coolant temperature. To stabilize this process, a feedback controller can be used to manipulate T_j directly.[57] Here, we design a jacketed CSTR by augmenting the system with energy balance in the jacket:[27]

$$\frac{dT_j}{dt} = \frac{F_j}{V_j}(T_{fj} - T_j) + \frac{UA}{\rho_j C_{pj} V_j}(T - T_j).$$

By performing the steady-state optimization on the augmented model, we seek to determine the reactor diameter $D \in [5, 15]$ and coolant flow rate $F_j \in [0, 150]$ that maximize the function:

$$\phi = 3342D^{1.868} + 120F_j$$

while satisfying the design constraints:

$$\begin{aligned} 0 \le \quad C_A \quad &\le 0.01, \\ 650 \le \quad T \quad &\le 725, \\ 650 \le \quad T_j \quad &\le 700. \end{aligned}$$

Parameters that are used in this study are summarized in Table 2.

In this example, we assume that uncertain parameters are $p = (C_{Af}, T_f, U)$ with $\bar{p} = (0.5, 530, 150)$ and $N = \bar{p} + [-0.05, 0.05] \times [-5, 5] \times [-5, 5]$ as in the table. By varying the feed flow rate F, we obtained the computational results in Table 3. For all the cases studied, robust stability is attained for free.

Table 3. Robust Solutions at Different Levels of F for the Jacketed CSTR Process

F	(D, F_j)	ϕ	Iteration #
50	(5, 37.674)	72,086	1
75	(5, 54.587)	74,116	1
100	(5, 72.977)	76,323	1
125	(5, 94.851)	78,948	1
150	(5, 118.536)	81,790	1

Ethanol Fermenter. The ethanol fermenter model compiled in Garhyan et al.[58] tracks the concentrations of the following components: substrate (C_S), product (C_P), biomass (C_X), and the internal key component (C_e):

$$\frac{dC_e}{dt} = \left(16 - 0.497C_P + 0.00383C_P^2\right)\frac{C_S C_e}{0.5 + C_S} - D_{in}C_e,$$
$$\frac{dC_X}{dt} = \frac{C_S C_e}{0.5 + C_S} - D_{in}C_X,$$
$$\frac{dC_S}{dt} = \frac{-100}{2.44498}\frac{C_S C_e}{0.5 + C_S} - 2.16C_X + D_{in}C_{S0} - D_{in}C_S,$$
$$\frac{dC_P}{dt} = \frac{100}{5.26315}\frac{C_S C_e}{0.5 + C_S} + 1.1C_X - D_{in}C_P.$$

Here, the manipulated variables $u' = (C_{S0}, D_{in})$ are uncertain. Therefore, we decompose $u' = u + p$ so that $u = (\overline{C}_{S0}, \overline{D}_{in})$ and $p = (\delta C_{S0}, \delta D_{in})$. The bounds X and U of these variables are given as:

$$C_e \le 0.5,\ C_X \le 5,\ 10 \le C_S \le 80,\ C_P \le 150,$$
$$0.01 \le D_{in} \le 0.1,\ 130 \le C_{S0} \le 150.$$

We optimize this system for ethanol yield Y_P subject to requirements on the substrate conversion X_S and the ethanol production rate per unit volume of the fermenter P_P, which are defined as follows:

$$\phi = Y_P = \frac{C_P - C_{P0}}{C_{S0}},$$
$$X_S = \frac{C_{S0} - C_S}{C_{S0}} \ge 0.84,$$
$$P_P = D_{in}C_P \ge 1.$$

For this problem, $Y(x)$ is taken to be the box of $\pm$ 10% of X around x. The 1% uncertainty case with $N = [-0.2, 0.2] \times [-0.0009, 0.0009]$ is solved in two iterations and 70.3 CPU s to give the optimal value of 0.4479 and the 2% case with $N = [-0.4, 0.4] \times [-0.0018, 0.0018]$ in three iterations and 128 CPU s to give the optimal value of 0.4477. The robust stability results are shown in Figure 5. As seen in this figure, the uncertainty boxes surrounding optimal solutions touch the stability boundary. The objective value increases as we move toward the lower left corner. Thus, the point-wise stable solution is at the intercept of the stability boundary with the line of $C_{S0} = 130$.

Continuous Polymerization Process. We consider a dynamic model for the free radical homopolymerization of vinyl acetate in solution[59]:

$$\frac{dT}{dt} = \frac{\rho_f C_{pf}}{\rho C_p}(T_f - 298) - \frac{\rho_f}{\rho}(T - 298) - \theta\frac{\rho_m \Delta H k_p P v_m}{\rho C_p W_m} - \theta\frac{\alpha B}{\rho C_p}(T - T_c),$$
$$\frac{dv_m}{dt} = \frac{\rho_{mf}}{\rho_m}(1 - v_{sf}) - \frac{q_{\text{out}}}{q_{\text{in}}}v_m - \theta\frac{W_m R_m}{\rho_m} - \frac{d\rho_m/dT}{\rho_m}\frac{dT}{dt}v_m,$$
$$\frac{dv_s}{dt} = \frac{\rho_{sf}}{\rho_s}v_{sf} - \frac{q_{\text{out}}}{q_{\text{in}}}v_s - \frac{d\rho_s/dT}{\rho_s}\frac{dT}{dt}v_s,$$
$$\frac{dI}{dt} = I_f - \frac{q_{\text{out}}}{q_{\text{in}}}I - \theta k_d I,$$

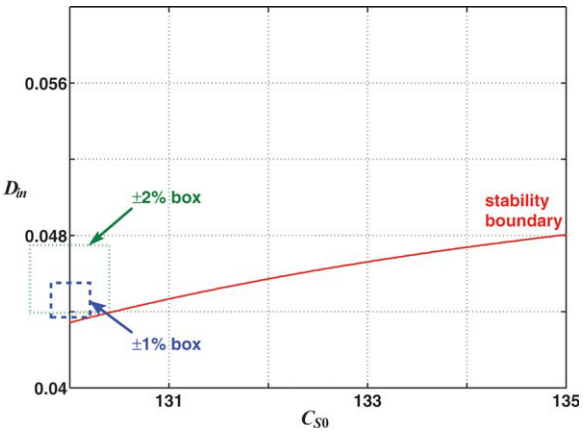

Figure 5. Robustly stable solutions for the ethanol fermenter.

[Color figure can be viewed in the online issue, which is available at wileyonlinelibrary.com.]

where T is the reactor temperature, v_m is the volume fraction of monomer, v_s is the volume fraction of solvent, and I is the initiator concentration. In the model, α, B, ΔH, W_m, W_s, W_i are constants, and C_p, ρ_m, ρ_s, ρ, k_d, k_p, P, R_m, $\frac{q_{\text{out}}}{q_{\text{in}}}$ are functions of state variables.[60]

Here, we assume that T_f, T_c, and v_{sf} are given, thus ρ_{mf}, ρ_{sf}, ρ_f and C_{pf} are fixed. We optimize feed initiator concentration I_f and residence time θ to maximize the following simplified profit function[29]:

$$\phi = \frac{-3\rho_{mf}(1 - v_{sf}) - \rho_{sf}v_{sf} - 360W_i I_f + 18\rho_p(1 - v_m - v_s)}{\theta}.$$

Variables are bounded so that $I_f \in (0, 0.1]$, $\theta \in (0, 200]$, $T \in [300, 500]$, $v_m \in [0, 0.5]$, $v_s \in [0.5, 1]$, and $I \in [0, I_f]$. The optimum operating condition $(I_f, \theta) = (0.0264, 0.772)$ corresponds to three possible steady states, one of which achieves the maximum objective value:

$$(T, v_m, v_s, I) = (430, 0.114, 0.646, 0.00153),\ \phi = 1980.$$

If we restrict $T \le 373$,[29] then we obtain

$$(I_f, \theta; T, v_m, v_s, I) = (0.0072, 6.01; 373, 0.225, 0.626, 0.0046),\ \phi = 173.$$

These solutions are obtained in 1.5 CPU min.

It is apparent that a higher temperature is preferred to maximize conversion. However, these high temperatures are not realistic considering the boiling point of the mixture that is close to 348. Therefore, we introduce an additional temperature constraint $T \le 348$. Moreover, we require robust stability under uncertainty in the design variables:

$$N:\ \delta\theta^2 + \left(1000\delta I_f\right)^2 \le 50$$

We consider the steady state x to be robustly stable if there exists at least one stable steady state in its neighborhood, $Y(x)$, for each realization of uncertain parameters in N. We take $Y(x)$ to be the same as X except that the temperature is within $\pm$ 10 of the operating temperature. The

Table 4. Solutions to the CSTR Polymerization Model

Requirements	(I_f, θ)	(T, v_m, v_s, I)	ϕ
No stability	(0.012, 54.2)	(348, 0.144, 0.64, 0.00983)	40.5
Point stability	(0.0264, 169)	(330, 0.136, 0.64, 0.0255)	9.2
Robust stability	(0.0277, 181)	(330, 0.13, 0.641, 0.0269)	8.72

solution to the problem is obtained in four iterations and 6 min and is summarized in Table 4 and Figure 6. We observed that the newly introduced stability constraints do not translate into a substantial increase in the solution time of the relaxation problem. Panel (a) shows the steady-state manifold near the optimal solutions. Blue points correspond to stable steady states while the white region corresponds to unstable steady states. In panel (b), robustly stable solution is shown with stability neighborhood touching the stability boundary. Overall, shorter residence time and faster conversion are preferable for faster processing and better objective, but stability demands longer and slower dynamics.

Tryptophan biosynthesis in bacteria

We consider a dynamic model for tryptophan biosynthesis in bacteria:[61]

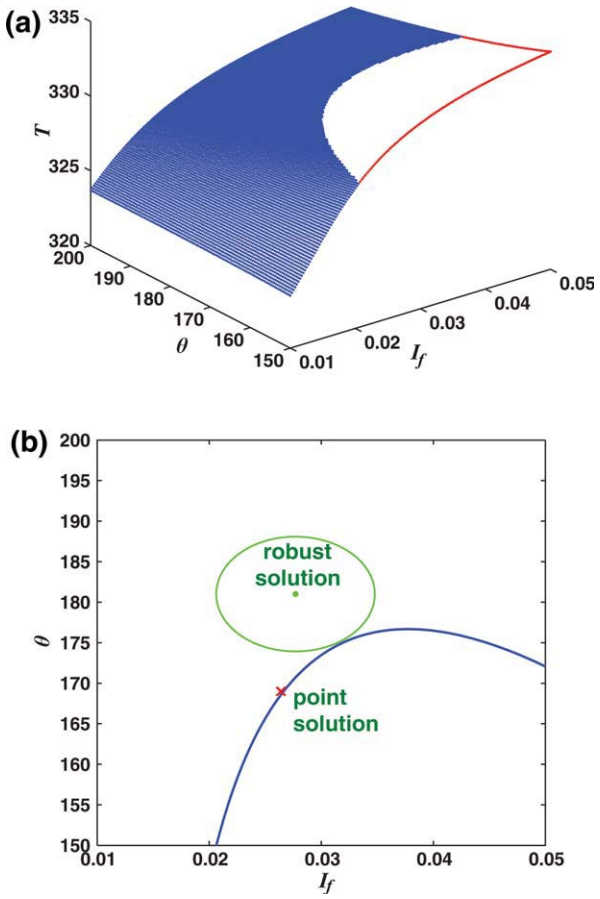

Figure 6. Computational results for the polymerization process.

[Color figure can be viewed in the online issue, which is available at wileyonlinelibrary.com.]

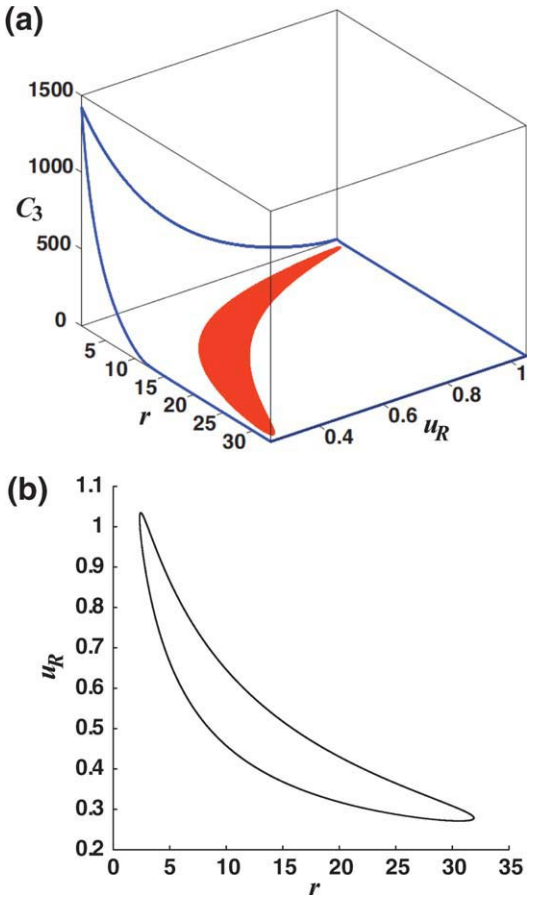

Figure 7. Steady-state manifold for the tryptophan synthesis model.

[Color figure can be viewed in the online issue, which is available at wileyonlinelibrary.com.]

$$\frac{dC_1}{dt} = \frac{1 + C_3}{1 + (1 + r)C_3} - (0.9 + v)C_1,$$

$$\frac{dC_2}{dt} = C_1 - (0.02 + v)C_2,$$

$$\frac{dC_3}{dt} = \frac{2283^2 C_2}{2283^2 + C_3^2} - vC_3 - \frac{0.024C_3}{1 + C_3} - \frac{430(1 - 7.5v)vC_3}{0.005 + C_3},$$

$$v = 0.0312u_R,$$

where state variables $x = (C_1, C_2, C_3)$ are used for the concentration of mRNA, enzyme, and tryptophan, respectively. The design variables $u' = (r, u_R)$ represent genetic and environmental controls.

We assume that r and u_R are uncertain, and decompose u' into $u = (\bar{r}, \bar{u}_R)$ and $p = (\delta r, \delta u_R)$. Variable bounds are given as $X = [0.1, 0.6] \times [4, 11] \times [0, 1]$ and $U = [5, 20] \times [0.5, 1]$. We take $N = [-0.15, 0.15] \times [-0.005, 0.005]$, which corresponds to 1% of the entire range of U. Figure 7 shows the steady-state manifold of this model on the 3D space of r, u_R, and C_3 and the projection of the stability boundary onto the 2D space of r and u_R. The white region in panel (a) corresponds to stable steady states. Panel (b) shows the stability boundary projected onto the parameter space. The crescent-shaped region corresponds to unstable steady states.

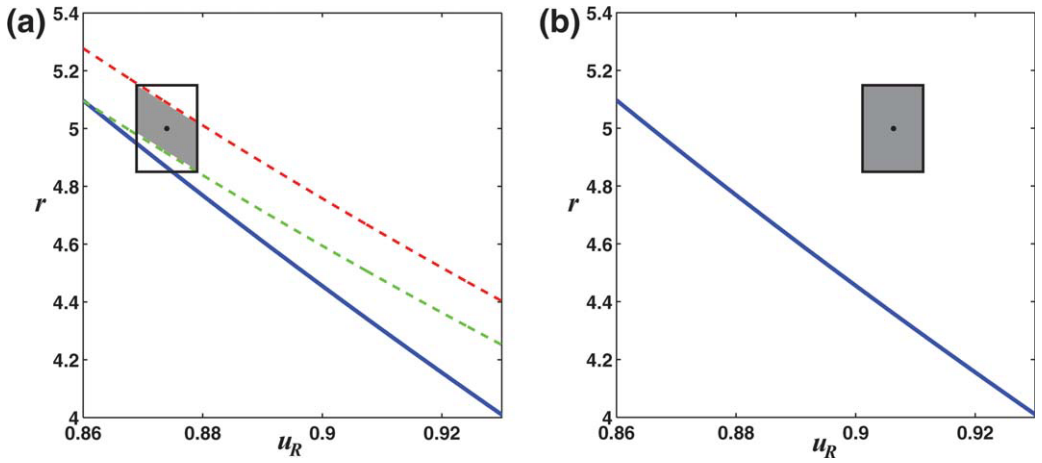

Figure 8. The original solution of Chang and Sahinidis[31] (left) and the most conservative solution (right) to the tryptophan synthesis problem.

[Color figure can be viewed in the online issue, which is available at wileyonlinelibrary.com.]

This model was solved in Chang and Sahinidis[31] based on the following assumptions:

- The real steady state could be different from the solution to the given ODE model due to an oversimplification of the underlying dynamics and parametric uncertainty.
- In spite of modeling errors, the Jacobian of the model can be used to determine the local stability of the real operating point.
- The uncertainty for states is 1% of their entire state range, thus $Y'(x) = [x_1 \mp 0.005] \times [x_2 \mp 0.07] \times [x_3 \mp 0.01]$ in formulation 6.

Plotting the robust stability result of Chang and Sahinidis,[31] $(r, u_R) = (5, 0.874)$, on the parameter space gives the left graph of Figure 8. In this graph, the blue solid line is the stability boundary, while the red and green dotted lines correspond to the level curves of $C_3 \pm 0.01$. Here, only the steady states in the shaded region (instead of the entire black box) are required to be stable.

Let us assume that we want to ensure that all the steady states in the black box are stable. Then, as in Gerhardt et al.,[32] we find the tightest possible $Y'(x)$ that does not compromise the uncertainty neighborhood N:

$$-0.0036 \le y_1 - x_1 \le 0.0036,$$
$$-0.0515 \le y_2 - x_2 \le 0.0514,$$
$$-0.0801 \le y_3 - x_3 \le 0.0931.$$

Using these bounds, the approach of Chang and Sahinidis[31] gives the following solution point:

$$x = (0.4572, 9.4704, 0.3722), \quad u = (5, 0.9063).$$

This solution is plotted on the parameter space as the right graph of Figure 8, which shows that the nearer the solution is to the stability boundary, the better the objective value is.

If there exists parametric uncertainty only, then the previous solution is too conservative. Applying the solution algorithm proposed here, the following solution point is obtained in four major iterations:

$$x = (0.4404, 9.2794, 0.4079), \quad u = (5, 0.88).$$

Not surprisingly, the solution box now touches the stability boundary as in Figure 9. It must be emphasized that this solution is robust only to the prescribed parametric uncertainty. We can use the extended formulation P′ to account for general uncertainties considered in Chang and Sahinidis.[31]

Conclusions

In this work, a methodology was developed for steady-state system design in a way that ensures robust stability of the steady-state solution under parametric uncertainty. Steady-state optimization problems with stability constraints were formulated as semi-infinite optimization problems, following the symbolic determination of algebraic stability conditions. To solve the semi-infinite programs, we proposed a row and

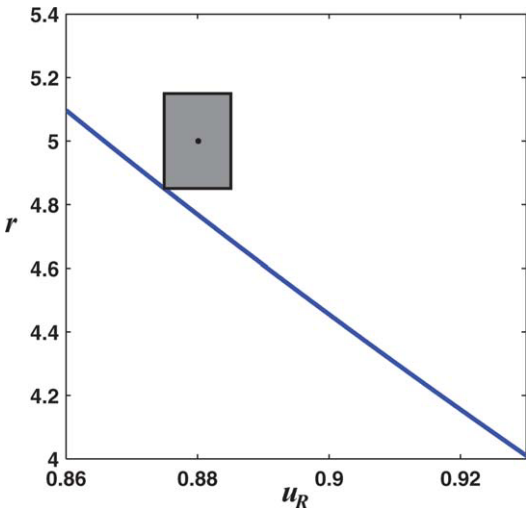

Figure 9. The steady-state solution to the tryptophan synthesis problem.

[Color figure can be viewed in the online issue, which is available at wileyonlinelibrary.com.]

column generation scheme, which adds a number of stability constraints and variables to a relaxation of the problem at each iteration, until the local stability condition is satisfied at all steady states within a prescribed uncertainty neighborhood. The proposed formulation and solution strategy was demonstrated by using it to predict the least conservative solutions for a variety of investigated examples, including fermentation processes, a polymerization process, and a biosynthesis process.

The proposed methodology comes with three unique features. First, it can handle nonsmooth or discontinuous uncertainty regions without overestimating them, thus guaranteeing the least conservative steady-state solutions that are robustly stable. Second, the method allows the redefinition of desired robustness in stability by way of bounding the state perturbations and tailoring the solution algorithm for multiple steady-state cases. Finally, our method can be applied to find stable limit-cycle solutions, which may be desired to increase process productivity via a deliberate unsteady operation of dynamic processes.

Since the proposed algorithm can be utilized to solve generalized semi-infinite programming problems of similar mathematical structure, investigating its performance in other application settings will constitute an interesting subject of future research.

Acknowledgment

The authors are thankful for partial financial support from the National Science Foundation under grant OCI-0750826.

Literature Cited

1. Biegler LT, Grossmann IE, Westerberg AW. *Systematic Methods of Chemical Process Design*. Upper Saddle River, NJ: Prentice Hall, 1997.
2. Seider WD, Brengel DD, Provost AM. Nonlinear analysis in process design. Why overdesign to avoid complex nonlinearities? *Ind Eng Chem Res*. 1990;5:806–818.
3. Swaney RE, Grossmann IE. An index for operational flexibility in chemical process design. Part I: formulation and theory. *AIChE J*. 1985;31:621–630.
4. Pistikopoulos EN, Mazzuchi TA. A novel flexibility analysis approach for processes with stochastic parameters. *Comput Chem Eng*. 1987;11:675–693.
5. Lai SM, Hui CW. Measurement of plant flexibility. *Comput Aided Chem Eng*. 2007;24:189–194.
6. Georgakis C, Uztürk D, Subramanian S, Vinson DR. On the operability of continuous processes. *Control Eng Pract*. 2003;11:835–971.
7. Lima FV, Jia Z, Ierapetritou M, Georgakis C. Similarities and differences between the concepts of operability and flexibility: the steady-state case. *AIChE J*. 2010;56:702–716.
8. Seferlis P, Georgiadis MC, editors. *The Integration of Process Design and Control*. Amsterdam: Elsevier, 2004.
9. Malcolm A, Polan J, Zhang L, Ogunnaike BA, Linninger AA. Integrating systems design and control using dynamic flexibility analysis. *AIChE J*. 2007;53:2048–2061.
10. Hamid MKA, Sin G, Gani R. Integration of process design and controller design for chemical processes using model-based methodology. *Comput Chem Eng*. 2010;34:683–699.
11. Bansal V, Perkins JD, Pistikopoulos EN, Ross R, van Schijndel JMG. Simultaneous design and control optimisation under uncertainty. *Comput Chem Eng*. 2000;24:261–266.
12. Li P, Arellano-Garcia H, Wozny G. Chance constrained programming approach to process optimization under uncertainty. *Comput Chem Eng*. 2008;32:25–45.
13. Ricardez-Sandoval LA, Budman HM, Douglas PL. Simultaneous design and control of processes under uncertainty: a robust modelling approach. *J Process Control*. 2008;18:735–752.
14. Ricardez-Sandoval LA, Budman HM, Douglas PL. Integration of design and control for chemical processes: a review of the literature and some recent results. *Annu Rev Control*. 2009;33:158–171.
15. LaSalle JP, Lefschetz S. *Stability by Liapunov's Direct Method with Applications*. New York: Academic Press, 1961.
16. Murty KG, Kabadi SN. Some NP complete problems in quadratic and nonlinear programming. *Math Program*. 1987;39:117–129.
17. Khalil HK. *Nonlinear Systems*, *3rd ed*. Upper Saddle River, NJ: Prentice Hall, 2002.
18. Davis RH, Kraemer E. An optimization procedure based on analytic stability conditions for systems linearized by the describing function method. *Appl Math Model*. 1982;6:16–22.
19. Kokossis AC, Floudas CA. Stability in optimal design: synthesis of complex reactor networks. *AIChE J*. 1994;40:849–861.
20. Nikolaev EV. The elucidation of metabolic pathways and their improvements using stable optimization of large-scale kinetic models of cellular systems. *Metab Eng*. 2010;12:26–38.
21. Hassibi A, How J, Boyd S. A path-following method for solving BMI problems in control. *Proceedings of the American Control Conference*, San Antonio, CA 1999;1385–1389.
22. Frazer RA, Duncan WJ. On the criteria for the stability of small motions. *P R Soc London A*. 1929;124:642–654.
23. Nemirovski A. Several NP-hard problems arising in robust stability analysis. *Math Control Signal*. 1993;6:99–105.
24. Toker O. On the complexity of the robust stability problem for linear parameter varying systems. *Automatica*. 1997;33:2015–2017.
25. Matsuda T, Mori T. Stability feeler: a tool for parametric robust stability analysis and its applications. *IET Control Theory A*. 2009;3:1625–1633.
26. Mohideen MJ, Perkins JD, Pistikopoulos EN. Robust stability considerations in optimal design of dynamic systems under uncertainty. *J Process Control*. 1997;7:371–385.
27. Blanco AM, Bandoni JA. Interaction between process design and process operability of chemical processes: an eigenvalue optimization approach. *Comput Chem Eng*. 2003;27:1291–1301.
28. Dobson I. Distance to bifurcation in multidimensional parameter space: Margin sensitivity and closest bifurcations. *Lect Notes Control Inf*. 2004;293:49–66.
29. Mönnigmann M, Marquardt W. Steady-state process optimization with guaranteed robust stability and feasibility. *AIChE J*. 2003;49:3110–3126.
30. Lu XJ, Li HX, Chen CLP. Robust optimal design with consideration of robust eigenvalue assignment. *Ind Eng Chem Res*. 2010;49:3306–3315.
31. Chang Y, Sahinidis NV. Optimization of metabolic pathways under stability considerations. *Comput Chem Eng*. 2005;29:467–479.
32. Gerhard J, Mönnigmann M, Marquardt W. Steady state optimization with guaranteed stability of a tryptophan biosynthesis model. *Comput Chem Eng*. 2008;32:2914–2919.
33. Colson B, Marcotte P, Savard G. An overview of bilevel optimization. *Ann Oper Res*. 2007;153:235–256.
34. Ierapetritou MG, Acevedo J, Pistikopoulos EN. An optimization approach for process engineering problems under uncertainty. *Comput Chem Eng*. 1996;20:703–709.
35. Lyapunov AM. The general problem of the stability of motion. *Int J Control*. 1992;55:531–534.
36. Chang Y, Sahinidis NV. Global optimization in stabilizing controller design. *J Global Optim*. 2007;38:509–526.
37. Hurwitz A. *On the conditions under which an equation has only roots with negative real parts*. In: Bellman RE, Kalaba R, editors. *Selected Papers on Mathematical Trends in Control Theory*. New York: Dover, 1964:72–82.
38. Gradshteyn IS, Ryzhik IM. *Table of Integrals, Series, and Products*, 7th ed. San Diego, CA: Academic Press, 2007.
39. Prigogine I, Lefever R. Symmetry breaking instabilities in dissipative systems. II. *J Chem Phys*. 1968;48:1695–1700.
40. Bahri PA, Bandoni JA, Romagnoli JA. Effect of disturbances in optimizing control: steady-state open-loop backoff problem. *AIChE J*. 1996;42:983–994.
41. Bahri PA, Bandoni JA, Romagnoli JA. Integrated flexibility and controllability analysis in design of chemical processes. *AIChE J*. 1997;43:997–1015.

42. Brendel M, Marquardt W. An algorithm for multivariate function estimation based on hierarchically refined sparse grids. *Comput Visual Sci*. 2009;12:137–153.
43. Bansal V, Perkins JD, Pistikopoulos EN. Flexibility analysis and design using a parametric programming framework. *AIChE J*. 2002;48:2851–2868.
44. Sahinidis NV. BARON: a general purpose global optimization software package. *J Global Optim*. 1996;8:201–205.
45. Tawarmalani M, Sahinidis NV. A polyhedral branch-and-cut approach to global optimization. *Math Program*. 2005;103:225–249.
46. Douglas JM, Rippin DWT. Unsteady state process operation. *Chem Eng Sci*. 1966;21:305–315.
47. Suman B. Study of unsteady state process operation. *Chem Eng J*. 2004;104:63–71.
48. Poincaré H. Mémoire sur les courbes définiés par une équation differentielle I. *J Math Pure Appl III*. 1881;7:375–422.
49. Liu L, Thomas JP, Dowell EH, Attar P, Hall KC. A comparison of classical and high dimensional harmonic balance approaches for a Duffing oscillator. *J Comput Phys*. 2006;215:293–320.
50. Seydel R. *Practical Bifurcation and Stability Analysis*, 3rd ed. New York: Springer, 2010.
51. Jalili-Kharaajoo M, Araabi BN. The Schur stability via the Hurwitz stability analysis using a biquadratic transformation. *Automatica*. 2005;41:173–176.
52. Agrawal P, Lee C, Lim HC, Ramkrishna D. Theoretical investigations of dynamic behavior of isothermal continuous stirred tank biological reactors. *Chem Eng Sci*. 1982;37:453–462.
53. Brengel DD, Seider WD. Coordinated design and control optimization of nonlinear processes. *Comput Chem Eng*. 1992;16:861–886.
54. Mönnigmann M, Marquardt W. Normal vectors on manifolds of critical points for parametric robustness of equilibrium solutions of ODE systems. *J Nonlinear Sci*. 2002;12:85–112.
55. Marquardt W, Mönnigmann M. Constructive nonlinear dynamics in process systems engineering. *Comput Chem Eng*. 2005;29:1265–1275.
56. Uppal A, Ray WH, Poore AB. On the dynamic behavior of continuous stirred tank reactors. *Chem Eng Sci*. 1974;29:967–985.
57. Hahn J, Mönnigmann M, Marquardt W. A method for robustness analysis of controlled nonlinear systems. *Chem Eng Sci*. 2004;59:4325–4338.
58. Garhyan P, Elnashaie SSEH, Al-Haddad SM, Ibrahim G, Elshishini SS. Exploration and exploitation of bifurcation/chaotic behavior of a continuous fermentor for the production of ethanol. *Chem Eng Sci*. 2003;58:1479–1496.
59. Teymour F, Ray WH. The dynamic behavior of continuous polymerization reactors—VI. Complex dynamics in full-scale reactors. *Chem Eng Sci*. 1992;47:4133–4140.
60. DeCicco J. Simulation of an industrial polyvinyl acetate CSTR and semi-batch reactor utilizing MATLAB and SIMULINK: version 1.0. Available at: http://citeseerx.ist.psu.edu/viewdoc/summary?doi=10.1.1.48.875. 1998.
61. Xiu ZL, Zeng AP, Decker WD. Model analysis concerning the effects of growth rate and intracellular tryptophan level on the stability and dynamics of tryptophan biosynthesis in bacteria. *J Biotechnol*. 1997;58:125–140.

Manuscript received July 17, 2010, and revision received Dec. 2, 2010.